Origin of the Phonon Hall Effect in Rare-Earth Garnets

Michiyasu Mori,[1] Alexander Spencer-Smith,[2] Oleg P. Sushkov,[3] and Sadamichi Maekawa[1]
[1]*Advanced Science Research Center, Japan Atomic Energy Agency, Tokai 319-1195, Japan*
[2]*School of Physics, University of Sydney, Sydney, New South Wales 2006, Australia*
[3]*School of Physics, University of New South Wales, Sydney, New South Wales 2052, Australia*
(Received 3 July 2014; published 22 December 2014)

The phonon Hall effect has been observed in the paramagnetic insulator $Tb_3Gd_5O_{12}$. A magnetic field applied perpendicularly to a heat current induces a temperature gradient that is perpendicular to both the field and the current. We show that this effect is due to resonant skew scattering of phonons from the crystal field states of superstoichiometric Tb^{3+} ions. This scattering originates from the coupling between the quadrupole moment of Tb^{3+} ions and the lattice strain. The estimated magnitude of the effect is consistent with experimental observations at $T \sim 5$ K and can be significantly enhanced by increasing temperature.

DOI: 10.1103/PhysRevLett.113.265901 PACS numbers: 66.70.-f, 72.20.Pa, 72.15.Gd

When a linear magnetic field is applied perpendicularly to a heat current in a sample of terbium gallium garnet (TGG) $Tb_3Ga_5O_{12}$, a transverse temperature gradient is induced in the third perpendicular direction [1,2]. This is the "phonon Hall effect" (PHE). The effect was observed in this insulator at low temperature ($T \sim 5$ K), a situation in which there are no mobile charges such as electrons or holes [3]. The Neél temperature of TGG is 0.24 K [4], so it is a paramagnet at $T \sim 5$ K. Hence, magnons do not contribute to the heat current and one does not expect a contribution from the magnon Hall effect [5–8]. Phonons are not charged and hence cannot be affected by the Lorentz force which gives rise to the usual classical Hall effect. Therefore, the mechanism for the PHE must be related to the spin-orbit interaction. However, the spin-orbit interaction for phonons is not at all obvious, unlike in the anomalous Hall effect and spin Hall effect for electrons [9–11]. Thus, an understanding of the origin of the observed PHE is a fundamental problem.

So far, there have been a few theoretical attempts to explain the PHE [12–15]. References [12] and [13] assumed a Raman-type interaction between the spin of stoichiometric Tb^{3+} ions and the phonon. This interaction results in "elliptically polarized" phonons. According to Refs. [12,13], the "elliptic polarization," in combination with scattering from impurities, leads to the PHE. In this scenario, the type of impurity is unimportant, and hence, phonon-impurity scattering is considered in the leading Born approximation. This is an intrinsic-extrinsic scenario; i.e., the elliptic polarization is an intrinsic effect and the scattering from impurities is an extrinsic effect. The major problem with this scenario was realized in Ref. [14]—in spite of the elliptic polarization, the Born approximation does not result in the PHE. Reference [14] attempted to go beyond the leading Born approximation in impurity scattering. However, the problem has not been resolved yet. An intrinsic mechanism for the PHE, based on the Berry curvature of phonon bands, was suggested in Ref. [15]. This is similar to the Berry curvature mechanism in the Hall effect for light [16]. The Berry curvature mechanism is certainly valid for materials with specially structured phonon bands; however, it is hard to see how the mechanism can be realized in TGG, which has the simple cubic structure.

There is an important experimental observation which was missed in all the previous theoretical analyses of the PHE—TGG crystals can be grown by the flux method (TGG_{fl}) and by the Czochralski method (TGG_G). While TGG_{fl} has perfect stoichiometry, TGG_G contains about 1% of superstoichiometric Tb^{3+} ions. At 5 K, the diagonal thermal conductivity of TGG_G is about 5 times smaller than that of TGG_{fl} [17]. This indicates that the thermal conductivity in TGG_G is determined by phonon scattering from the crystal field states of superstoichiometric Tb^{3+} ions [17]. The PHE has only been observed in TGG_G [1,2]. Thus, one concludes that the PHE is of extrinsic origin—due to the phonon scattering from superstoichiometric Tb^{3+} ions. We stress that the PHE in TGG relies specifically upon scattering from superstoichiometric Tb^{3+} ions, not just scattering from any impurities. This observation was not considered in all previous suggestions [12,13,15] for the mechanism behind the PHE.

In this Letter, motivated by the above observation, we show that the PHE originates from the resonant skew scattering of phonons from the crystal field states of superstoichiometric Tb^{3+} ions. Below, we will often refer to superstoichiometric Tb^{3+} ions as impurities.

Phonons.—The phonon Lagrangian density reads

$$\mathcal{L}_0 = \frac{\rho}{2}\{\dot{\varphi}_j^2 - c_T^2(\partial_i\varphi_j)^2 - (c_L^2 - c_T^2)(\partial_i\varphi_i)(\partial_j\varphi_j)\},$$
$$\boldsymbol{\varphi} = \sum_{\boldsymbol{q},\mu} \frac{\boldsymbol{e}_\mu}{\sqrt{2\rho\omega_{\boldsymbol{q}\mu}}}[a_{\boldsymbol{q}\mu}e^{-i\omega_{\boldsymbol{q}\mu}t+i\boldsymbol{q}\cdot\boldsymbol{r}} + \text{H.c.}]. \quad (1)$$

Here, $\boldsymbol{\varphi}$ is lattice displacement. The isotropic model (1) is known to be appropriate for a system with a large unit cell, such as that of a garnet [18–20]. The index $\mu = 1, 2, 3$ enumerates phonon polarization, $\boldsymbol{e}^{(\mu)}$ is the unit polarization vector, $a_{\boldsymbol{q}\mu}$ is the annihilation operator of the phonon, and $\omega_{\boldsymbol{q}\mu} = c_L q (c_T q)$ is the energy of the longitudinal (transverse) phonon. For the purpose of making estimates, we will use the following value of speed $c \approx 3.7 \times 10^5$ cm/s and the mass density $\rho = 7.2$ g/cm^3 [17]. Below, only the longitudinal mode is considered. It is plausible that this mode dominates the PHE due to its large velocity $c_L \approx 2c_T$ [19]. Even if transverse modes gave comparable contributions, this does not influence our estimate of the effect.

Tb ion.—The $^7F_6$state of a free Tb^{3+} ion splits into 13 levels in the dodecahedral crystal field of the garnet. The energies of low lying levels in intrinsic ions are approximately 0, 3, 49, 62, 72, and 76 K [21,22]. The energy levels of impurity ions (superstoichiometric) depend on their particular positions, but overall, they are comparable to those of ions in regular sites. The thermal conductivity in TGG_G is mainly determined by the resonant scattering of phonons from superstoichiometric ions. Note that resonant scattering necessarily implies a nonzero scattering phase and hence gives rise to skew scattering, which does not appear in the Born approximation [23].

Fitting the measured diagonal thermal conductivity [17] within four levels of the impurity ion, we come to the ion level scheme shown in the left-hand side of Fig. 1: $\omega_{ab} = 3$ K, $\omega_{ac} = 20$ K, $\omega_{ad} = 70$ K (see the Supplemental Material [24]). It is known that the ground state energy doublet is very sensitive to magnetic field B. At $T = 4.2$ K and $B < 1$ T, the ion magnetic moment grows linearly with B. At fields larger than 1–2 T, the magnetic moment practically saturates at $|M| \approx 4\mu_B$ [25]. These data indicate that the a, b states are composed of time conjugate states $|\pm M\rangle$, $|a\rangle \propto |+M\rangle + |-M\rangle$, $|b\rangle \propto |+M\rangle - |-M\rangle$, and, subjected to a magnetic field, the a, b states evolve to $|\pm M\rangle$ as shown in the right-hand side of Fig. 1: $\omega_{ab} \to \Omega_{a'b'} = \sqrt{\omega_{ab}^2 + (2gB)^2}$ with an effective g factor [26]. Below, we assume that, for the magnetic field larger than 1–2 T, only the state $|a'\rangle = |+M\rangle$ is thermally populated, while, without magnetic field, both $|a\rangle$ and $|b\rangle$ are populated. For simplicity, we assume that $|c\rangle$ and $|d\rangle$ are not sensitive to the magnetic field.

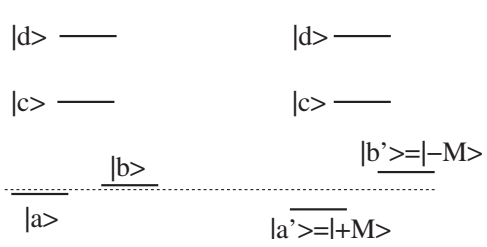

FIG. 1. The crystal field levels for $B = 0$ on the left and for $B >$ 1–2 T on the right.

Spin-phonon interaction.—The quadrupole Coulomb interaction of a Tb ion with its surrounding lattice ions is of the following form [27,28]:

$$H_1 = \gamma T_{ij} \partial_i \varphi_j,$$
$$T_{ij} = \frac{3}{2J(2J-1)} \left\{ J_i J_j + J_j J_i - \frac{2}{3} J(J+1)\delta_{ij} \right\}. \quad (2)$$

Here, φ_j is the lattice displacement at the ion site $i, j = x, y, z$. The quadrupole moment $Q_{ij} = QT_{ij}$ is written in terms of the total angular momentum J. This implies that the strong spin-orbit interaction inside the ion core is embedded in Eq. (2). The size of an ion core is about one Bohr radius a_B. Hence, the quadrupole moment Q is roughly estimated as $Q \sim ea_B^2$, where e is the elementary charge. The gradient of the electric field E from the surrounding ions is estimated as $\nabla E \sim e/d^3$, where $d \approx 2$ Å is the distance to the nearest oxygen ion. Then, the magnitude of the coupling γ is

$$\gamma \sim Q \nabla E \sim \frac{e^2 a_B^2}{d^3} \sim 0.7 \text{ eV}. \quad (3)$$

Resonant scattering.—Phonon scattering from superstoichiometric Tb^{3+} ions is determined by the diagram in Fig. 2. Under nonzero magnetic field, a straightforward calculation gives the following scattering rate for a phonon with energy ω:

$$\tau_\omega^{-1} = \tau_L^{-1} + \sum_{i=b',c,d} \tau_{a'i,\omega}^{-1},$$
$$\tau_{a'i,\omega}^{-1} = \frac{N_s}{N_{\text{Tb}}} \frac{\omega_D^3 \omega^4}{80\pi} \frac{(\Omega_{a'i}/\omega_{ai})^2 \Gamma_{ai}^2/\omega_{ai}^4}{(\omega^2 - \Omega_{a'i}^2)^2 + \Omega_{a'i}^2 \Gamma_{i\omega}^2},$$
$$\Gamma_{ai} = \gamma^2 \omega_{ai}^3/\pi\rho c^5, \qquad \Gamma_{i\omega} = (\omega/\omega_{ai})^3 \Gamma_{ai}. \quad (4)$$

Here, $\tau_L^{-1} = c/L$ is due to the finite size of the sample $L \approx 1$ mm. The total density of Tb ions is $N_{\text{Tb}} \approx 1.3 \times 10^{22}$ cm^{-3}, the density of superstoichiometric Tb ions is $N_s \approx 1.5 \times 10^{20}$ cm^{-3}, and the Debye frequency or temperature is $\omega_D = 487$ K [17]. Equation (4) is similar to that derived a long time ago in Refs. [29,30]. It is worth

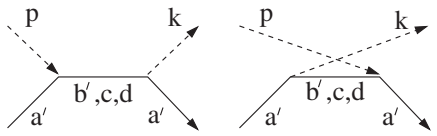

FIG. 2. Amplitude of phonon scattering from a Tb ion with virtual excitation of the crystal field level given a magnetic field larger than 1–2 T. The solid line shows the ionic state, and the dashed line shows the phonon. Without the magnetic field, the initial state a' is substituted by the states a or b, with c and d as intermediate states.

noting that the ω^4 dependence in the numerator of the resonant part of τ_ω^{-1} originates from the derivative in the interaction (2). This derivative is enforced by Adler's theorem [31].

Skew component.—We take the magnetic field directed along the z axis. The phonon propagates in the xy plane with an initial momentum $\boldsymbol{k} = k(1,0,0)$ and final momentum $\boldsymbol{q} = k(\cos\phi, \sin\phi, 0)$, where ϕ is the scattering angle. When the magnetic field is small, the states a' and b' are populated and then the diagrams in Fig. 2 give the following phonon angular distributions for scattering (see Ref. [32] and the Supplemental Material [24]):

$$W^{a'c}_{\boldsymbol{k}\to\boldsymbol{q}} \approx \frac{\tau^{-1}_{a'c,\omega}}{2\pi}\left(\cos^2\phi - \frac{\omega\Gamma_{c\omega}}{\Omega^2_{a'c}}\cos\phi\sin\phi\right), \quad (5)$$

$$W^{b'c}_{\boldsymbol{k}\to\boldsymbol{q}} \approx \frac{\tau^{-1}_{b'c,\omega}}{2\pi}\left(\cos^2\phi + \frac{\omega\Gamma_{c\omega}}{\Omega^2_{b'c}}\cos\phi\sin\phi\right). \quad (6)$$

Note that the second term proportional to $\sin\phi$ is the skew component and the sign of the $a'c$ process is opposite to that of the $b'c$ process. This is due to the time conjugation of the states $|a'\rangle = |+M\rangle$ and $|b'\rangle = |-M\rangle$. Without the magnetic field, these process cancel each other out, whereas with a magnetic field, the skew component becomes finite for two reasons—the energy difference between $\Omega_{a'c}$ and $\Omega_{b'c}$, and the depopulation of the state b'. The $a'b'$ and $b'a'$ processes also contribute to scattering such as Eqs. (5) and (6), respectively. If the states a' and b' are equally populated, the skew components in these processes cancel each other out, since $\tau_{a'b',\omega} = \tau_{b'a',\omega}$ and $|\Omega_{b'a'}| = |\Omega_{a'b'}|$. When the state b' is depopulated by increasing the magnetic field, the cancellation becomes imperfect and the $a'b'$ process also contributes to the skew scattering.

Correlation of impurity positions.—The $\cos\phi\sin\phi$ term in Eqs. (5) and (6) changes sign at $\phi \to -\phi$. This is the skew asymmetry which is necessary for the PHE. However, this term also changes sign at $\phi \to \pi - \phi$. Because of this, the off-diagonal thermal conductivity is 0 ($\kappa_{xy} = 0$), in spite of the skew, since skew scattering in the forward hemisphere $\cos\phi > 0$ is exactly compensated for by skew scattering in the backward hemisphere $\cos\phi < 0$. There is no such problem for electron skew scattering [33], but there is a similar problem for the skew scattering of light. There are two mechanisms which destroy the $\phi \to \pi - \phi$ compensation: (i) the spatial correlation of impurity positions discussed below and (ii) interference between contributions with different values of ΔJ_z; this mechanism is discussed in the Supplemental Material [24].

A superstoichiometric Tb^{3+} ion has ionic radius 0.92 Å and it replaces a Ga^{3+} ion with smaller radius 0.62 Å. Hence, the crystal lattice around the Tb ion is elastically deformed towards larger lattice spacing. During the process of crystal growth, this creates more room for another superstoichiometric Tb ion in the vicinity of the first one. Hence, the impurity density $\rho_s(\boldsymbol{r})$ must be correlated as

$$\overline{\rho_s(0)\rho_s(\boldsymbol{r})} = N_s\delta(\boldsymbol{r}) + N_s^2[1 + Ce^{-r/l}], \quad (7)$$

where the correlation length is about the average distance between impurities $l \approx N_s^{-1/3} \approx 2\times10^{-7}$ cm. Given the significant difference in ionic radii, it is natural to assume about a 50% change in the probability of having another superstoichiometric Tb ion in the vicinity of the first one. Hence, it is reasonable to expect that the correlation constant is $C \sim \pm 1$. Because of the correlation (7), the interference between phonon scattering amplitudes from adjacent impurities is nonzero and the scattering probability [Eq. (5)] is modified by an interference term as $W_{k\to q} \to W_{k\to q}(1 + CP_\phi)$, where $P_\phi = 1/[1 + (2kl\sin\phi/2)^2]^2$. Thus, the correlation destroys the $\phi \to \pi - \phi$ compensation factor. It is convenient to expand P_ϕ in a series of Legendre polynomials $P_\phi = a_0(\omega) + a_1(\omega)P_1(\cos\phi) + \cdots$, where

$$a_1(\omega) = \frac{3}{(\omega/\omega_1)^2}\left[1 + \frac{1}{1+(\omega/\omega_1)^2}\right] - \frac{6}{(\omega/\omega_1)^4}\ln[1 + (\omega/\omega_1)^2] \quad (8)$$

and $\omega_1 \equiv \hbar c/2l \approx 13$ K. Hence, accounting for mechanism (i) (see also the Supplemental Material [24]), the scattering rate given by Eqs. (5) and (6) is transformed to

$$W_{\boldsymbol{k}\to\boldsymbol{q}} \approx \frac{\tau_\omega^{-1}}{4\pi}\{1 - \mathcal{K}_\omega\omega\Gamma_{c\omega}\boldsymbol{n}_B\cdot[\boldsymbol{n}_k\times\boldsymbol{n}_q]\},$$
$$\mathcal{K}_\omega = \frac{C}{5}a_1(\omega)\tau_\omega\left(\frac{\tau^{-1}_{a'c,\omega}}{\Omega^2_{a'c}} - n_T\frac{\tau^{-1}_{b'c,\omega}}{\Omega^2_{b'c}} + \bar{n}_T\frac{\tau^{-1}_{a'b',\omega}}{\Omega^2_{a'b'}}\right),$$
$$n_T \equiv \exp[-\Omega_{a'b'}/T] \equiv 1 - \bar{n}_T, \quad (9)$$

where $\boldsymbol{n}_B, \boldsymbol{n}_k, \boldsymbol{n}_q$ are unit vectors along the direction of the magnetic field and the phonon momenta, respectively, and n_T and $\bar{n}_T$ are the thermal populations.

Phonon Hall effect.—The Boltzmann equation for the phonon distribution function $f_k = f_k^{(0)} + g_k^{(S)} + g_k^{(A)}$ reads [34]

$$c^2\mathbf{k}\cdot\left(\frac{\nabla T}{T}\right)\left(-\frac{\partial f_{\boldsymbol{k}}^{(0)}}{\partial\omega_k}\right) \approx \sum_q (W_{\boldsymbol{q}\to\boldsymbol{k}}f_{\boldsymbol{q}} - W_{\boldsymbol{k}\to\boldsymbol{q}}f_{\boldsymbol{k}}). \quad (10)$$

Here, $f_k^{(0)}$ is the equilibrium Bose-Einstein distribution. Since the scattering rate (9) contains both the symmetric part $W^{(S)}_{q\to k} = W^{(S)}_{k\to q}$ and the asymmetric part $W^{(A)}_{q\to k} = -W^{(A)}_{k\to q}$, we need to account for the two nonequilibrium components $g_k^{(S)}$ and $g_k^{(A)}$:

$$g_k^{(S)} \propto (\boldsymbol{k}\cdot\nabla T), \qquad g_k^{(A)} \propto (\boldsymbol{k}\cdot[\boldsymbol{n}_B\times\nabla T]). \quad (11)$$

Assuming that the asymmetry parameter in Eq. (9) is small $\mathcal{K}_\omega \omega \Gamma_{c\omega} \ll 1$, the solution of the Boltzmann equation is straightforward and results in the following nonequilibrium part of the distribution function

$$g_k^{(S)} + g_k^{(A)} = -\frac{e^{\omega_k/T}}{(e^{\omega_k/T}-1)^2}\frac{c^2}{T^2}\tau_\omega \times \left\{(\boldsymbol{k}\cdot\nabla T) - \frac{1}{3}\mathcal{K}_\omega \omega \Gamma_\omega (\boldsymbol{k}\cdot[\boldsymbol{n}_B \times \nabla T])\right\}. \quad (12)$$

Hence, we calculate the diagonal and the off-diagonal thermal conductivities as

$$\kappa_{xx} = \frac{T^3}{2\pi^2 c}\int \tau_\omega \frac{x^4 e^x dx}{(e^x-1)^2}, \quad (13)$$

$$\kappa_{xy} = \frac{T^3}{2\pi^2 c}\int \tau_\omega \frac{\mathcal{K}_\omega}{3}\omega\Gamma_\omega \frac{x^4 e^x dx}{(e^x-1)^2}, \quad (14)$$

where $x \equiv \omega/T$. The diagonal thermal conductivity in Eq. (13) is of the standard form [35], which is used to fit the data in Ref. [17]. The transverse thermal conductivity κ_{xy} given by Eq. (14) is shown in Fig. 3 as a function of T with $B = 1, 2, 3$ T. We can see that κ_{xy} is enhanced by T and B (see also the inset in Fig. 3). Note that this result is justified for $T < \Omega_{a'c} \sim 20$ K since the state c is assumed to be unpopulated. The inset in Fig. 3 is the B dependence of κ_{xy}, which increases and finally starts to decrease around $B \sim 2.5$ T.

Our estimate of the phonon Hall angle S immediately follows from Eqs. (13) and (14) and, for magnetic fields larger than 1–2 T, is

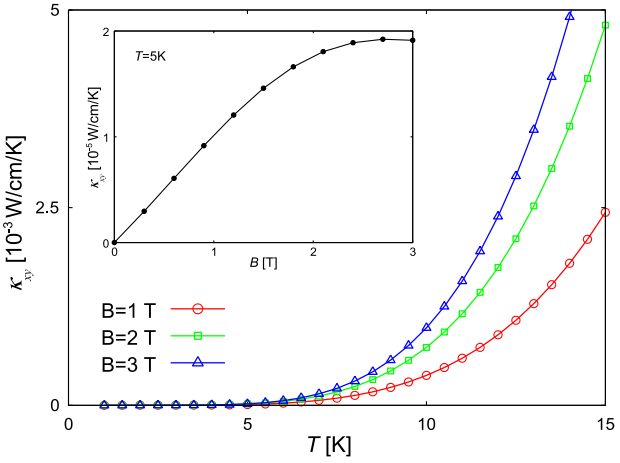

FIG. 3 (color online). Magnetic field dependence of the transverse component of thermal conductivity κ_{xy} (10^{-3} W/cm/K). The inset is the magnetic field dependence of κ_{xy} (10^{-5} W/cm/K) at $T = 5$ K. Here, $g = 1$ and $\omega_{ab} = 0$, and the state d is ignored.

$$S \equiv \frac{1}{B}\frac{\kappa_{xy}}{\kappa_{xx}}. \quad (15)$$

Assuming that at temperature $T = 5$ K the frequency is $\omega = T = 5$ K, Eq. (15) results in the following estimate: $S(T = 5\text{ K}) \sim 5 \times 10^{-4}$ rad/T. An accurate evaluation of the integrals in Eq. (13) confirms that the primary contribution to κ_{xx} comes from $\omega \approx T = 5$ K. On the other hand, the dominant contribution to κ_{xy} comes from $\omega \sim 30$ K—the phonon Hall effect is due to relatively "hot" phonons. Accounting for the hot phonon effect enhances our theoretical estimate: $S(T = 5\text{ K}) \sim 10^{-3}$ rad/T. Our estimate is reasonably consistent with measurements $S(T = 5.45\text{ K}) \approx 1 \times 10^{-4}$ rad/T [1] and $S(T = 5.13\text{ K}) \approx 0.35 \times 10^{-4}$ rad/T [2]. The presented theoretical estimates of κ_{xy} correspond to $C \sim 1$. It is important that the C dependence of the Hall angle may explain the significant difference between the two measurements; i.e., two different crystals were used in the two measurements [1,2] (see also the Supplemental Material [24]).

Conclusion.—We have shown that the puzzling phonon Hall effect observed in $Tb_3Gd_5O_{12}$ is due to the resonant skew scattering of phonons from the crystal field levels of superstoichiometric Tb^{3+} ions. The obtained magnitude of the effect is in agreement with experiments performed at $T = 5$ K. We predict that the magnitude of the effect grows very significantly with temperature in the interval $3\text{ K} < T < 15$ K. Compared to the performed measurements, we expect the effect to be about an order of magnitude larger at $T = 10$–15 K. A mechanism similar to that considered here for the phonon Hall effect is also valid for the Hall effect of light [36]: skew scattering of light from atomic or molecular transitions. For light, the quadrupole crystal field interaction [Eq. (2)] should be replaced by the electric dipole interaction.

We would like to thank A. I. Milstein, G. Khaliullin, G. Jackeli, C. Ulrich, and M. Fujita for stimulating discussions. This work was supported by the Grant-in-Aid for Scientific Research and the bilateral program from MEXT. M. M. thanks the Godfrey Bequest and the School of Physics at the University of New South Wales for financial support and kind hospitality. O. P. S. thanks the Japan Society for Promotion of Science and Advanced Science Research Centre JAEA for financial support and kind hospitality.

[1] C. Strohm, G. L. J. A. Rikken, and P. Wyder, Phys. Rev. Lett. **95**, 155901 (2005).
[2] A. V. Inyushkin and A. N. Taldenkov, JETP Lett. **86**, 379 (2007).
[3] Band gaps in garnets are about 5 eV; see, e.g., D. J. Robbins, B. Cockayne, B. Lent, and J. L. Glasper, Solid State Commun. **36**, 691 (1980).
[4] J. Hammann and M. Ocio, J. Phys. (Paris) **38**, 463 (1977).
[5] Y. Onose, Y. Shiomi, and Y. Tokura, Phys. Rev. Lett. **100**, 016601 (2008).

[6] H. Katsura, N. Nagaosa, and P. A. Lee, Phys. Rev. Lett. **104**, 066403 (2010).
[7] Y. Onose, T. Ideue, H. Katsura, Y. Shiomi, N. Nagaosa, and Y. Tokura, Science **329**, 297 (2010).
[8] R. Matsumoto and S. Murakami, Phys. Rev. Lett. **106**, 197202 (2011); R. Matsumoto and S. Murakami, Phys. Rev. B **84**, 184406 (2011).
[9] M. I. D'yakonov and V. I. Perel', Zh. Eksp. Teor. Fiz. Pis. Red. **13**, 657 (1971) [JETP Lett. **13**, 467 (1971)].
[10] J. E. Hirsch, Phys. Rev. Lett. **83**, 1834 (1999).
[11] For a review see S. Maekawa, *Concepts in Spin Electronics* (Oxford University Press, Oxford, England, 2006).
[12] L. Sheng, D. N. Sheng, and C. S. Ting, Phys. Rev. Lett. **96**, 155901 (2006).
[13] Yu. Kagan and L. A. Maksimov, Phys. Rev. Lett. **100**, 145902 (2008).
[14] L. A. Maksimov and T. V. Khabarova, Dokl. Akad. Nauk SSR **442**, 749 (2012) [Dokl. Phys. **57**, 51 (2012)].
[15] L. Zhang, J. Ren, J.-S. Wang and B. Li, Phys. Rev. Lett. **105**, 225901 (2010); L. Zhang, J. Ren, J.-S. Wang., and B. Li, J. Phys. Condens. Matter **23**, 305402 (2011); T. Qin, J. Zhou, and J. Shi, Phys. Rev. B **86**, 104305 (2012).
[16] M. Onoda, S. Murakami, and N. Nagaosa, Phys. Rev. Lett. **93**, 083901 (2004).
[17] A. V. Inyushkin and A. N. Taldenkov, Zh. Eksp. Teor. Fiz. **138**, 862 (2010) [JETP **111**, 760 (2010)].
[18] C. Kittel, *Introduction to Solid State Physics* (Wiley, New York, 1966).
[19] J. S. Plant, J. Phys. C **10**, 4805 (1977).
[20] Throughout this Letter, we set both Planck's constant and Boltzmann's constant equal to unity: $\hbar = k_B = 1$.
[21] J. A. Koningstein and C. J. Kane-Maguire, Can. J. Chem. **52**, 3445 (1974).
[22] J. Hammann and P. Manneville, J. Phys. (Paris) **34**, 615 (1973).
[23] L. D. Landau and E. M. Lifshitz, *Quantum Mechanics Non-Relativistic Theory* (Butterworth-Heinemann, Oxford, 1981), 3rd ed., Vol. 3.
[24] See Supplemental Material at http://link.aps.org/supplemental/10.1103/PhysRevLett.113.265901 for the thermal conductivity of TGG and some technical details.
[25] N. P. Kolmakova, R. Z. Levitin, A. I. Popov, N. F. Vedernikov, A. K. Zvezdin, and V. Nekvasil, Phys. Rev. B **41**, 6170 (1990).
[26] The $|\pm M\rangle$ states are composed of states with definite z projection of the ion angular momentum J such as $|+M\rangle = \cdots|+2\rangle + \alpha_+|+1\rangle + \alpha_0|0\rangle + \alpha_-|-1\rangle + \cdots$ and $|-M\rangle = \cdots|-2\rangle - \alpha_+|-1\rangle + \alpha_0|0\rangle - \alpha_-|+1\rangle + \cdots$.
[27] A. A. Abragam and B. Bleaney, *Electron Paramagnetic Resonance of Transition Ions* (Clarendon, Oxford, England, 1970).
[28] P. Fulde, *Handbook on the Physics and Chemistry of Rare Earths* (North-Holland, Oxford, 1979), Vol. 2, p. 295.
[29] F. W. Sheard and G. A. Toombs, Solid State Commun. **12**, 713 (1973).
[30] G. A. Toombs and F. W. Sheard, J. Phys. C **6**, 1467 (1973).
[31] S. L. Adler, Phys. Rev. **137**, B1022 (1965).
[32] In the skew part, we account only for the virtual c state and neglect the virtual d state. This is because $\Gamma_{d\omega}/\Omega_{ad}^2 \ll \Gamma_{c\omega}/\Omega_{ac}^2$, and hence, the skew component for the d state is relatively small.
[33] A. Fert, J. Phys. F **3**, 2126 (1973).
[34] W. Kohn and J. M. Luttinger, Phys. Rev. **108**, 590 (1957).
[35] R. Berman, *Thermal Conduction in Solids* (Clarendon, Oxford, England, 1976).
[36] G. L. J. A. Rikken and B. A. van Tiggelen, Nature (London) **381**, 54 (1996).